ACS Energy LETTERS

http://pubs.acs.org/journal/aelccp

Erschienen in: ACS Energy Letters ; 1 (2016), 2. - S. 438-444
https://dx.doi.org/10.1021/acsenergylett.6b00236

LETTER

Photoluminescence Lifetimes Exceeding 8 μs and Quantum Yields Exceeding 30% in Hybrid Perovskite Thin Films by Ligand Passivation

Dane W. deQuilettes, Susanne Koch,[†] Sven Burke, Rajan K. Paranji, Alfred J. Shropshire, Mark E. Ziffer, and David S. Ginger*

Department of Chemistry, University of Washington, Box 351700, Seattle, Washington 98195-1700, United States

Supporting Information

ABSTRACT: We study the effects of a series of post-deposition ligand treatments on the photoluminescence (PL) of polycrystalline methylammonium lead triiodide perovskite thin films. We show that a variety of Lewis bases can improve the bulk PL quantum efficiency (PLQE) and extend the average PL lifetime, $\langle\tau\rangle$, with large enhancements concentrated at grain boundaries. Notably, we demonstrate thin-film PLQE as high as 35 ± 1% and $\langle\tau\rangle$ as long as 8.82 ± 0.03 μs at solar equivalent carrier densities using tri-*n*-octylphosphine oxide-treated films. Using glow discharge optical emission spectroscopy and nuclear magnetic resonance spectroscopy, we show that the ligands are incorporated primarily at the film surface and are acting as electron donors. These results indicate it is possible to obtain thin-film PL lifetime and PLQE values that are comparable to those from single crystals by control over surface chemistry.

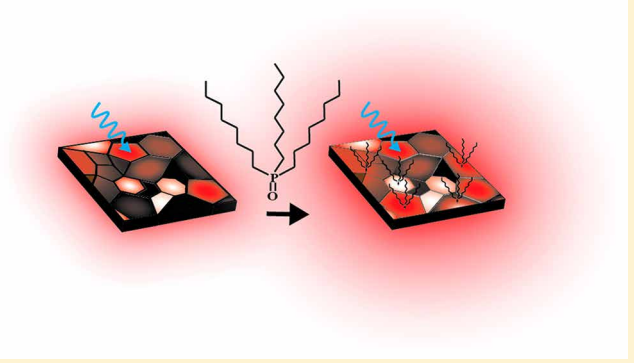

Organic−inorganic trihalide perovskites are a family of earth-abundant semiconductors with composition-tunable bandgaps that exhibit promising performance in a range of electronic and optoelectronic devices including solar cells, light-emitting diodes, lasers, and ambipolar transistors.[1−3] Recently, high-quality perovskite single crystals have been grown using a variety of techniques and demonstrate exceptional optoelectronic properties that surpass their polycrystalline counterparts.[4−6] In particular, it has been shown that single crystals possess lower defect concentrations, higher mobilities, longer carrier diffusion lengths, and longer carrier lifetimes,[4−6] suggesting that the surface defects that are more prevalent in polycrystalline films limit performance.[7−9] Despite the quality of single crystals, their growth can be time-consuming and their structural properties make them more difficult to incorporate into many devices, particularly those requiring large areas such as solar cells. Therefore, there is still significant interest in processing perovskites rapidly from solution into polycrystalline thin films for device applications. Many studies have highlighted the "defect tolerance" of perovskites, underlining their apparent resistance to defects that would normally plague semiconductors processed at low temperature.[10,11] While the performance of hybrid perovskite devices may be surprisingly good for a low-temperature, solution-processed thin-film technology, polycrystalline perovskite films still operate well below their theoretical performance limits, indicating that losses remain. Indeed, we recently used photoluminescence (PL) microscopy to reveal a subset of grain boundaries and "dark" regions in the films that serve as nonradiative centers, highlighting the role of heterogeneity and surface effects.[12,13] Consistent with these studies, it has been shown that photoluminescence quantum efficiency (PLQE) and lifetime are limited by traps at carrier densities obtained under typical solar illumination, and only at high carrier densities (when the majority of traps are filled) are the highest PLQEs observed.[14−17] These observations help explain why the carrier lifetimes and PLQEs of thin films of perovskites remain below those reported for single crystals[2,7,8,18,19] and suggest that surface defect chemistry remains an important topic of study.[7,9,20,21]

Historically, controlling the surface chemistry in semiconductors such as Si and GaAs has been important in improving material properties for the development of solar cell technologies.[22−24] In II−VI and IV−VI quantum dot systems, a substantial amount of work has focused on ligand passivation to modify surface states to improve PL emission properties as well as solar cell efficiencies.[25−29]

Received: June 28, 2016
Accepted: July 26, 2016
Published: July 26, 2016

DOI: 10.1021/acsenergylett.6b00236
ACS Energy Lett. 2016, 1, 438−444

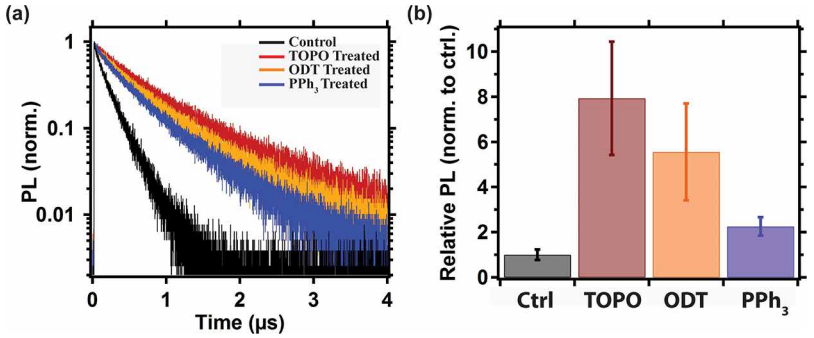

Figure 1. Photoluminescence studies of films treated with Lewis bases. (a) Bulk time-resolved photoluminescence decay traces of control (black) film treated with trioctylphosphine oxide (TOPO, red), octadecanethiol (ODT, orange), and triphenylphosphine (PPh_3, blue), excited with pulsed excitation (470 nm, 125 kHz repetition rate, 30 nJ/cm^2 per pulse). (b) Integrated PL intensity statistics of control and TOPO-, ODT-, and PPh_3-treated films. Error bars are standard error of the mean for N = 20.

In an effort to increase the photoluminescence quantum efficiency and lifetime in perovskites, several groups have utilized Lewis bases and acids to reduce defect densities and improve solar cell device performance.[14,21,30−33] For example, we recently found that pyridine vapor exposure to as-grown films can improve PL brightness while partially homogenizing the heterogeneous local PL emission.[12] Other reports have incorporated Lewis bases and acids into perovskite precursor solutions before film deposition to improve performance.[30−33] However, it has been difficult to assess whether the additives lead to better crystallization and growth of the films[30−32] or if their residual presence in the film ameliorates nonradiative recombination.[31,32] Recently, Li et al. proposed that alkylphosphonic acid ω-ammonium chlorides can hydrogen bond with iodine atoms at the surface to improve grain cohesivity and device performance while also noting the beneficial role passivation may have in long-term device stability.[32] Chen et al. have controlled the formation of PbI_2 at grain boundaries to reduce recombination at surface states,[34] while Asbury and coworkers showed that small dithiols could remove surface defects.[21]

Herein, we study the effect of post-deposition treatments with a variety of Lewis bases on the photoluminescence behavior of methylammonium lead triiodide perovskite thin films. We find that Lewis bases generally enhance the PL properties and can boost PL lifetimes nearly an order of magnitude to values as high as 8.82 ± 0.03 μs, the longest PL lifetime measured to date for thin films. Concomitant with improvements in lifetime, treated films also exhibit PLQE values as high as 35 ± 1% at solar equivalent carrier densities. We use fluorescence imaging to show that these improvements are concentrated at the grain boundaries. Using glow discharge optical emission spectroscopy (GDOES) and nuclear magnetic resonance (NMR) spectroscopy, we confirm that these treatments behave in a fashion consistent with an electron-donating surface layer, rather than structure-directing agents. This work identifies quick and facile post-deposition methods to improve materials processing and the quality of perovskite films. Further optimization of passivation schemes and a better understanding of perovskite surface chemistry could allow solution-processed polycrystalline films to approach the electronic quality of single crystals.

We prepared neat perovskite films on glass by spin-coating a precursor solution containing $PbOAc_2{\cdot}3H_20$ and MAI in *N*,*N*-dimethylformamide (DMF) following the work of Zhang et al. (see the Supporting Information for full details).[35] We then exposed these films to a variety of thiols, amines, phosphines, and phosphine oxides and studied their impact on PL properties. We treated the films with low concentration (0.005−0.087 M) solutions of different ligands dissolved in chlorobenzene (CB) by spin-coating the ligand solutions onto the perovskite thin films (see the Supporting Information). To improve reproducibility, as well as exclude the effects that small amounts of water and oxygen can impart on the PL, we prepared, treated, and measured all samples in dry nitrogen (see the Supporting Information).[36−38]

Figure 1a shows typical bulk time-resolved PL decay traces measured at low pump fluence (470 nm, 30 nJ/cm^2 per pulse, corresponding to an excitation density of ∼10^{15} cm^{-3}) of several samples before and after single chemical treatments with tri-*n*-octylphosphine oxide (TOPO), 1-octadecanethiol (ODT), and triphenylphosphine (PPh_3) measured in nitrogen. These compounds are all expected to behave as monodentate ligands because they possess only one coordinating atom. We also investigated some bidentate ligands as well as various other coordinating atoms, all of which showed general improvements in the PL (see Figure S1 for all treatments explored). Before ligand treatment, the PL lifetimes are typically of the order of a hundred nanoseconds, consistent with high-quality $CH_3NH_3PbI_3$ films reported by a number of authors.[21,39,40] Figure 1 shows that all of the screened treatments extend both the PL lifetime and the integrated PL intensity (Figure 1b) of the perovskite films, suggesting that the treatments are removing nonradiative decay pathways. To determine if this observation extends to different perovskite preparation routes, we performed these same treatments on films prepared using $PbCl_2$ and PbI_2 as Pb sources and observed similar improvements (Figure S2). We note that control films exposed to only neat CB solution do not show improvements in PL (Figure S3) and also that treated films washed with CB or 2-propanol can, depending on the washing procedure, result in a reinitialization of the PL intensity (Figure S4). This data suggests that the ligands are relatively labile and can be removed by rinsing with a suitable solvent.

Next, we examine the interaction between the potential ligands and the perovskite thin films. First, we used glow discharge optical emission spectroscopy (GDOES) to probe the chemical composition as a function of depth for samples treated with the thiol, ODT. This technique has been employed to detect small dopant concentrations (ppm) in thin films of a-Si:H and other semiconductors, making it capable of probing the small concentrations of molecules introduced onto the

DOI: 10.1021/acsenergylett.6b00236
ACS Energy Lett. 2016, 1, 438−444

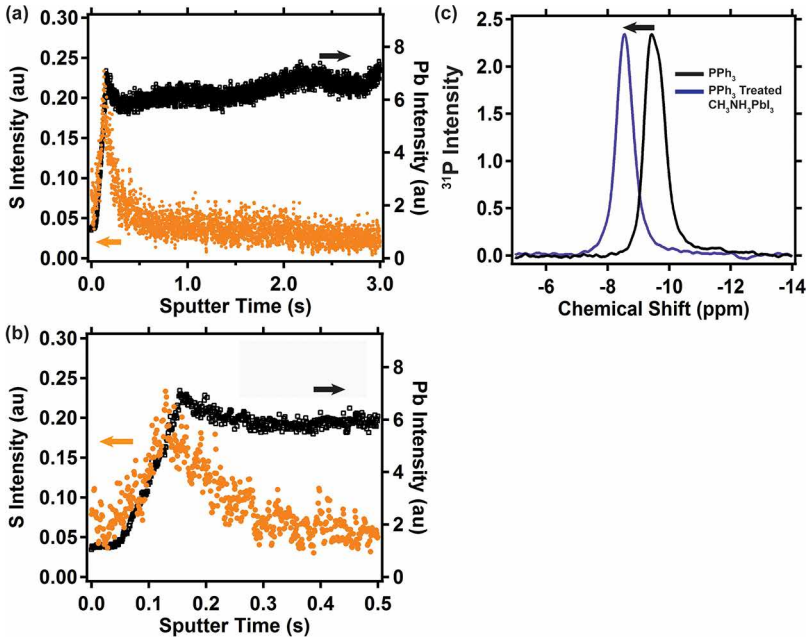

Figure 2. Evidence that Lewis bases are acting as surface ligands. (a) GDOES plot of an octadecanethiol (ODT)-treated film monitoring the sulfur (S, orange) and lead (Pb, black) intensities as a function of film depth. (b) Plot identical to that shown in panel a with a shorter sputter time window, highlighting the composition at the surface. (c) ^{31}P solid-state NMR spectroscopy of the free ligand triphenylphosphine (PPh_3, black) versus a perovskite sample treated with PPh_3 (blue).

perovskite surface.[41,42] Figure 2a,b shows the sulfur (S) and lead (Pb) intensities as a function of sputtering time (film depth) for a sample treated with 0.087 M ODT (see the Supporting Information for sample preparation). We observe a peak in the sulfur signal at the surface (i.e., onset of the Pb signal) of the ODT-treated film, which is not present in an untreated control film (Figure S5), indicating that ODT is primarily present at the film surface, not the bulk. We note that small concentrations of ODT may have penetrated further into the film (i.e., grain boundaries) but may be below the detection limit (ppm) of the technique.[41,42] We also confirmed that the treatments do not measurably change the optical density of the film or lead to measurable microscopic restructuring of the film morphology as evidenced by scanning electron microscopy (SEM) and X-ray diffraction (XRD) (Figures S6 and S7). The fact that the treatment is applied after film growth, that the ODT is confined to the surface, and that we see no other quantifiable changes in the film structure strongly suggests that the Lewis base is acting as a surface ligand rather than affecting the bulk structure.

To further verify whether the Lewis bases could be interacting with the perovskite surfaces as classic electron-donating ligands, we performed ^{31}P solid-state NMR spectroscopy on PPh_3-treated samples (see the Supporting Information for sample preparation). NMR spectroscopy gives insight into the local bonding environment of spin-active nuclei and has been widely employed to understand the surface chemistry of quantum dots.[26,43] Figure 2c shows that the phosphorus peak of a PPh_3-treated perovskite sample is shifted downfield when compared to the free ligand control. This downfield shift is consistent with the expected reduction in electron density surrounding the phosphorus nucleus (i.e., deshielding) upon interaction with the perovskite, which we take as confirmation that PPh_3 is indeed acting as an electron-donating molecule (Lewis base) and surface ligand.[43,44] Our results from solid-state NMR in conjunction with GDOES build a strong case that surface defects exist and can be passivated with post-deposition ligand treatments. Underscoring this result, we note that the ligands improve the PL while being confined nearly exclusively to the film surface as would be expected from their steric bulk and as experimentally confirmed by GDOES. Furthermore, the NMR data show that the compounds are acting as electron-donating ligands.

Having screened a range of different Lewis base treatments with our perovskite thin films, we next consider the PL enhancements that can be achieved with an optimized treatment. Figure 3a shows the champion time-resolved PL decay trace of a control film treated with 0.025 M TOPO dissolved in chlorobenzene and measured at a low fluence (470 nm, 50 nJ/cm^2 per pulse). The fits to the data are stretched exponential curves with a characteristic lifetime, τ_c = 0.92 ± 0.01 μs, and stretching exponent, β = 0.90, for the control and τ_c = 7.60 ± 0.04 μs and β = 0.77 for the TOPO-treated film. Error ranges for the PL lifetimes are estimated from the uncertainties in the fit parameters based on photon counting statistics, where the errors in the reported β values are negligible. This stretched exponential behavior at relatively low excitation power is consistent with literature reports[12,45,46] and indicative of a distribution of local monomolecular recombination rates resulting from heterogeneity in the local nonradiative decay rates.[12,13,20,47−50] We computed the average lifetime, $\langle\tau\rangle$, of the stretched exponential distribution according to eq 1:[51]

$$\langle\tau\rangle = \frac{\tau_c}{\beta}\Gamma\left(\frac{1}{\beta}\right) \tag{1}$$

where $\Gamma(1/\beta)$ is defined as the gamma function in eq 2:

$$\Gamma\left(\frac{1}{\beta}\right) = \int_0^\infty x^{(1-\beta)/\beta}\, e^{-x}\, dx \tag{2}$$

We obtained $\langle\tau\rangle$ = 0.97 ± 0.01 μs for the control film, which improved to $\langle\tau\rangle$ = 8.82 ± 0.03 μs when treated with TOPO,

DOI: 10.1021/acsenergylett.6b00236
ACS Energy Lett. 2016, 1, 438−444

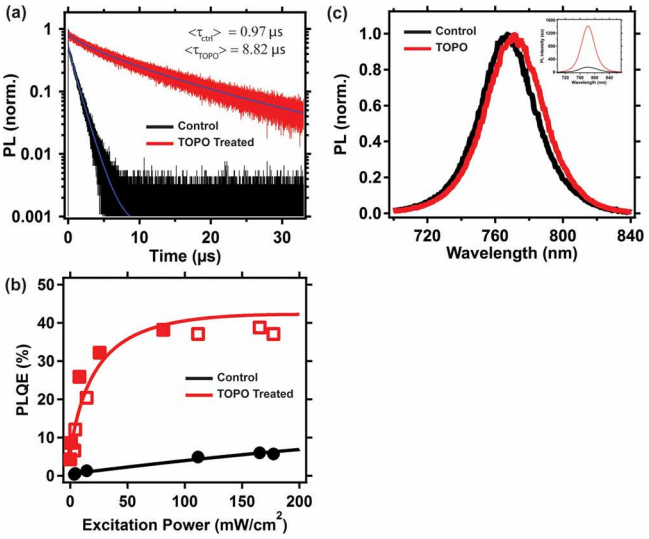

Figure 3. Photoluminescence measurements of optimized ligand treatment. (a) Champion bulk time-resolved photoluminescence (PL) decay traces of control (black) and trioctylphosphine oxide (TOPO, red) treated films on glass excited with pulsed excitation (470 nm, 30 kHz repetition rate, 50 nJ/cm^2 per pulse). (b) External PL quantum efficiency of films reported in panel a as a function of excitation power (532 nm, CW laser). Solid red squares are data taken 1 week prior to data marked with open squares, showing good sample stability. Solid lines are fits to the data taking into consideration monomolecular, bimolecular, and Auger recombination (see the Supporting Information). (c) Normalized steady-state photoluminescence spectrum of control (black) and TOPO (red) treated film and (inset) raw PL data, showing the relative intensities before and after TOPO treatment.

where error values are the propagated uncertainty in the input fit parameters. Figure 3b plots the PLQE of these same films measured in an integrating sphere as a function of excitation power. The data show that the PLQE increases roughly an order of magnitude for films treated with TOPO compared to control films across all excitation powers. Importantly, we find at excitation powers which generate carrier densities comparable to 1 sun illumination[52] that the PLQE can be enhanced from ∼3% for the control film to values as high as 35 ± 1% for the TOPO-treated film. The increase in PLQE as a function of excitation power has been attributed to increasing radiative bimolecular recombination as a result of trap filling.[15,16,52] Following previous reports,[16,52] we modeled the PLQE data using a combination of nonradiative and radiative monomolecular, bimolecular, and Auger recombination terms (see the Supporting Information and Figure S8). We report small variations in the radiative monomolecular, $k_r = 3.8 \times 10^4$ s^{-1}; bimolecular, $k_b = 4.0 \times 10^{-11}$ cm^3 s^{-1}; and Auger rate constants, $k_A = 4 \times 10^{-28}$ cm^6 s^{-1} for the treated film, compared to the control film, where $k_r = 4.1 \times 10^4$ s^{-1}, $k_b = 3.5 \times 10^{-11}$ cm^3 s^{-1}, and $k_A = 4 \times 10^{-28}$ cm^6 s^{-1}, which are consistent with literature values.[12,53,54] In contrast, we observe a significant difference in the nonradiative monomolecular rate constant, $k_{nr} = 9.1 \times 10^5$ s^{-1}, for the TOPO-treated film compared to $k_{nr} = 6.6 \times 10^6$ s^{-1} for the control film. This corresponds to a ∼7-fold reduction in the nonradiative decay rate for the TOPO-treated film, consistent with a comparable reduction in nonradiative recombination centers and nearly an order of magnitude increase in PLQE for the TOPO-treated film. We note that these rate constant values are consistent with our fitting of the TRPL data at low carrier densities (∼10^{15} cm^{-3}) to a superposition of monomolecular relaxation functions as we

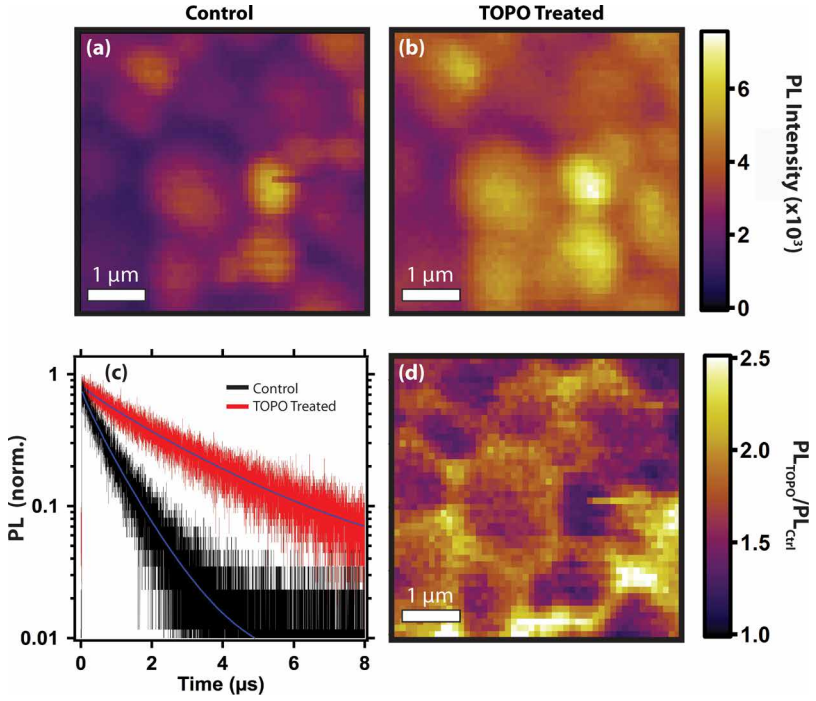

Figure 4. Fluorescence microscopy of ligand passivated film. (a) Fluorescence image of a perovskite film before (a) and after (b) trioctylphosphine oxide (TOPO) treatment plotted on the same PL intensity scale. (c) Bulk time-resolved photoluminescence of the control film (black) with an average lifetime ⟨τ⟩ = 0.73 ± 0.01 μs, which improved to 2.40 ± 0.09 μs after TOPO (red) treatment (470 nm, 125 kHz, 70 nJ/cm^2 per pulse). Solid lines are stretched exponential fits to the data. (d) Image showing the ratio of (b) TOPO-treated fluorescence image divided by (a) the control fluorescence image.

DOI: 10.1021/acsenergylett.6b00236
ACS Energy Lett. 2016, 1, 438−444

find, within this regime, that bimolecular recombination contributes to only ~5% of the total recombination rate in comparison to ~95% from monomolecular recombination.

To better elucidate the mechanism by which nonradiative recombination is reduced, we also performed steady-state PL spectroscopy. Figure 3c shows the PL spectra before and after TOPO treatment. We consistently observe a small red-shift for TOPO-treated films in comparison to the control films. Previously, our group has reported an improvement in PL and concomitant blue-shift in the optical features for pyridine-treated films,[12] which suggests treatments may modulate the electronic structure near the band-edge. Interestingly, it has been reported that large grain size polycrystalline films have a red-shifted PL peak compared to small grain polycrystalline films and also that single-crystal bulk emission is red-shifted compared to the surface emission.[9,17,55,56] These differences in the measured optical properties have been attributed to compositional changes at the grain boundaries, lattice strain, variations in crystallinity, and photon recycling.[9,17,55−57] Here we report no observable changes in XRD spectra or in average grain size (Figures S6) and minimal shift in the PL spectrum over long time scales (Figure S9), suggesting that the PL emission in our samples may be dominated, in part, by the surface composition.

Previously, we showed that pyridine homogenizes the PL of perovskite thin films.[12] Figure 4 shows a fluorescence intensity image of a control film before (Figure 4a) and after (Figure 4b) treatment with TOPO plotted on the same PL intensity scale. Overall we find that TOPO treatment has a similar effect as pyridine, generally enhancing PL in all regions of film, with grain boundaries still being generally dimmer than grain centers. This ensemble improvement is also evident from the enhancement in the average bulk lifetime (Figure 4c), where the control film initially exhibited $\langle\tau\rangle = 0.73 \pm 0.01$ μs which increased to $\langle\tau\rangle = 2.40 \pm 0.09$ μs after TOPO treatment. The measured bulk improvement can be further partitioned into local improvements. Figure 4d shows an image with the ratio of the PL intensity image for the TOPO-treated film to the control film. We find that the relative differential improvement at the grain boundaries (average enhancement factor of ~1.8×) is larger than for the grain centers (~1.6×), suggesting that the TOPO is preferentially active at passivating grain boundary surface states (Figure S10). More generally, we find that the largest improvements in PL are achieved for regions with initially lower PL, which we have previously correlated to regions of higher defect densities (Figure S10).[12,13] The preferential brightening of grain boundaries could result from the three-dimensional topography of grain boundaries, which may have higher defect densities than some of the flatter surfaces of the grain interiors or potentially the selective targeting of facet-dependent defect states.[58] Together these results are again broadly consistent with the picture that these treatments are reducing nonradiative recombination associated with surface states.

Reducing nonradiative recombination so that perovskite thin films can approach 100% photoluminescence quantum efficiency remains an important technological goal.[11,52,59,60] In the case where all nonradiative surface states were effectively passivated, we would expect the carrier lifetimes and PLQEs in polycrystalline films to approach that of single crystals.[2,7,18] To date, there has been a wide range of reported single-crystal carrier lifetimes spanning from tens of nanoseconds to hundreds of microseconds, depending on the measurement technique.[4−6,8,56] Polycrystalline films, on the other hand, do not typically exhibit microsecond carrier lifetimes but rather possess lifetimes ranging from tens of nanoseconds to a few hundred nanoseconds.[39,45,52] To the best of our knowledge, Noel et al. previously reported the longest measured PL lifetime for polycrystalline films to date, with values reaching ~2 μs upon surface treatment with pyridine and thiophene when measured at low fluence.[14] In addition to the long carrier lifetimes measured in this work, we also report PLQEs exceeding 30%. For polycrystalline thin films, PLQEs are typically ~10% or lower under excitation powers comparable to 1 sun illumination,[12,40,52,61,62] and only in single-crystal nanowires and nanocrystals are PLQEs in excess of 50% reached.[2,18,19] Our findings here suggest that the surface chemistry of polycrystalline films can be controlled to approach the carrier lifetimes and PLQEs more typical of single crystals.

After studying a library of Lewis bases, we have found that optimized treatments have reduced nonradiative recombination in $CH_3NH_3PbI_3$ perovskite films, extended PL lifetimes to values as high as 8.82 ± 0.03 μs, and improved PLQE values to 35 ± 1% at solar equivalent carrier densities. To further support the idea that these treatments are specifically targeting surface defects, we used glow discharge optical emission spectroscopy to show ligands are confined predominately at the film surface where steric effects likely prevent penetration further into the bulk of the film. With ^{31}P solid-state nuclear magnetic resonance, we showed that the molecules are behaving as classic surface ligands and Lewis bases. These results highlight the detrimental effect of perovskite surface states on optoelectronic performance, and here we show a facile and rapid post-deposition method that can alter the surface composition, yielding polycrystalline films with improved optoelectronic quality. With further development and characterization of ligand passivation schemes as well as a deeper understanding of their impact on the perovskite electronic structure, it is likely that thin-film perovskites will be able to approach their maximum theoretical performance in a wide range of polycrystalline perovskite optoelectronic devices.

■ ASSOCIATED CONTENT

Supporting Information

The Supporting Information is available free of charge on the ACS Publications website at DOI: 10.1021/acsenergylett.6b00236.

Materials and methods, supplementary text, photoluminescence measurements of other Lewis bases and precursor preparation routes, solvent wash control experiments, linear absorption spectroscopy, XRD spectroscopy, SEM characterization, streak camera experiments, and fluorescence image analysis (PDF)

■ AUTHOR INFORMATION

Corresponding Author

*E-mail: ginger@chem.washington.edu.

Present Address

†S.K.: Department of Physics, University of Konstanz, P.O. Box 680, 78457 Konstanz, Germany.

Notes

The authors declare no competing financial interest.

DOI: 10.1021/acsenergylett.6b00236
ACS Energy Lett. 2016, 1, 438−444

■ ACKNOWLEDGMENTS

D.W.D and D.S.G acknowledge DOE (DE-SC0013957) for supporting the local imaging work. D.W.D. acknowledges support from an NSF Graduate Research Fellowship (DGE-1256082) and thanks J. Mohammed, L. Bradshaw, G. Eperon, N. Li, and A. Marchioro for experimental help. This research was performed in part at the Molecular Analysis Facility (MAF), which is funded, in part, by the University of Washington, Molecular Engineering and Sciences Institute, and the Clean Energy Institute, as well as infrastructure grants from the National Institutes of Health (NIH) and the National Science Foundation (ECCS-1542101).

■ REFERENCES

(1) Stranks, S. D.; Snaith, H. J. Metal-Halide Perovskites for Photovoltaic and Light-Emitting Devices. *Nat. Nanotechnol.* **2015**, *10*, 391−402.

(2) Zhang, W.; Eperon, G. E.; Snaith, H. J. Metal Halide Perovskites for Energy Applications. *Nat. Energy* **2016**, *1*, 16048.

(3) Mei, Y.; Zhang, C.; Vardeny, Z. V.; Jurchescu, O. D. Electrostatic Gating of Hybrid Halide Perovskite Field-Effect Transistors: Balanced Ambipolar Transport at Room-Temperature. *MRS Commun.* **2015**, *5*, 297−301.

(4) Shi, D.; Adinolfi, V.; Comin, R.; Yuan, M.; Alarousu, E.; Buin, A.; Chen, Y.; Hoogland, S.; Rothenberger, A.; Katsiev, K.; et al. Low Trap-State Density and Long Carrier Diffusion in Organolead Trihalide Perovskite Single Crystals. *Science* **2015**, *347*, 519−522.

(5) Dong, Q.; Fang, Y.; Shao, Y.; Mulligan, P.; Qiu, J.; Cao, L.; Huang, J. Electron-Hole Diffusion Lengths > 175 μm in Solution-Grown $CH_3NH_3PbI_3$ Single Crystals. *Science* **2015**, *347*, 967−970.

(6) Saidaminov, M. I.; Abdelhady, A. L.; Murali, B.; Alarousu, E.; Burlakov, V. M.; Peng, W.; Dursun, I.; Wang, L.; He, Y.; Maculan, G.; et al. High-Quality Bulk Hybrid Perovskite Single Crystals Within Minutes by Inverse Temperature Crystallization. *Nat. Commun.* **2015**, *6*, 7586.

(7) Yang, Y.; Yan, Y.; Yang, M.; Choi, S.; Zhu, K.; Luther, J. M.; Beard, M. C. Low Surface Recombination Velocity in Solution-Grown $CH_3NH_3PbBr_3$ Perovskite Single Crystal. *Nat. Commun.* **2015**, *6*, 7961.

(8) Bi, Y.; Hutter, E. M.; Fang, Y.; Dong, Q.; Huang, J.; Savenije, T. J. Charge Carrier Lifetimes Exceeding 15 μs in Methylammonium Lead Iodide Single Crystals. *J. Phys. Chem. Lett.* **2016**, *7*, 923−928.

(9) Wu, B.; Nguyen, H. T.; Ku, Z.; Han, G.; Giovanni, D.; Mathews, N.; Fan, H. J.; Sum, T. C. Discerning the Surface and Bulk Recombination Kinetics of Organic-Inorganic Halide Perovskite Single Crystals. *Adv. Energy Mater.* **2016**, *6*, 1600551.

(10) Brandt, R. E.; Stevanović, V.; Ginley, D. S.; Buonassisi, T. Identifying Defect-Tolerant Semiconductors with High Minority-Carrier Lifetimes: Beyond Hybrid Lead Halide Perovskites. *MRS Commun.* **2015**, *5*, 265−275.

(11) Tvingstedt, K.; Malinkiewicz, O.; Baumann, A.; Deibel, C.; Snaith, H. J.; Dyakonov, V.; Bolink, H. J. Radiative Efficiency of Lead Iodide Based Perovskite Solar Cells. *Sci. Rep.* **2014**, *4*, 6071.

(12) deQuilettes, D. W.; Vorpahl, S. M.; Stranks, S. D.; Nagaoka, H.; Eperon, G. E.; Ziffer, M. E.; Snaith, H. J.; Ginger, D. S. Impact of Microstructure on Local Carrier Lifetime in Perovskite Solar Cells. *Science* **2015**, *348*, 683−686.

(13) deQuilettes, D. W.; Zhang, W.; Burlakov, V. M.; Graham, D. J.; Leijtens, T.; Osherov, A.; Bulovic, V.; Snaith, H. J.; Ginger, D. S.; Stranks, S. D. Photo-Induced Halide Redistribution in Organic-Inorganic Perovskite Films. *Nat. Commun.* **2016**, *7*, 11683.

(14) Noel, N. K.; Abate, A.; Stranks, S. D.; Parrott, E. S.; Burlakov, V. M.; Goriely, A.; Snaith, H. J. Enhanced Photoluminescence and Solar Cell Performance via Lewis Base Passivation of Organic-Inorganic Lead Halide Perovskites. *ACS Nano* **2014**, *8*, 9815−9821.

(15) Deschler, F.; Price, M.; Pathak, S.; Klintberg, L. E.; Jarausch, D. D.; Higler, R.; Huttner, S.; Leijtens, T.; Stranks, S. D.; Snaith, H. J.; et al. High Photoluminescence Efficiency and Optically Pumped Lasing in Solution-Processed Mixed Halide Perovskite Semiconductors. *J. Phys. Chem. Lett.* **2014**, *5*, 1421−1426.

(16) Stranks, S. D.; Burlakov, V. M.; Leijtens, T.; Ball, J. M.; Goriely, A.; Snaith, H. J. Recombination Kinetics in Organic-Inorganic Perovskites: Excitons, Free Charge, and Subgap States. *Phys. Rev. Appl.* **2014**, *2*, 034007.

(17) D'Innocenzo, V.; Srimath Kandada, A. R.; De Bastiani, M.; Gandini, M.; Petrozza, A. Tuning the Light Emission Properties by Band Gap Engineering in Hybrid Lead Halide Perovskite. *J. Am. Chem. Soc.* **2014**, *136*, 17730−17733.

(18) Zhu, H.; Fu, Y.; Meng, F.; Wu, X.; Gong, Z.; Ding, Q.; Gustafsson, M. V.; Trinh, M. T.; Jin, S.; Zhu, X. Y. Lead Halide Perovskite Nanowire Lasers with Low Lasing Thresholds and High Quality Factors. *Nat. Mater.* **2015**, *14*, 636−642.

(19) Protesescu, L.; Yakunin, S.; Bodnarchuk, M. I.; Krieg, F.; Caputo, R.; Hendon, C. H.; Yang, R. X.; Walsh, A.; Kovalenko, M. V. Nanocrystals of Cesium Lead Halide Perovskites ($CsPbX_3$, X = Cl, Br, and I): Novel Optoelectronic Materials Showing Bright Emission with Wide Color Gamut. *Nano Lett.* **2015**, *15*, 3692−3696.

(20) Bischak, C. G.; Sanehira, E. M.; Precht, J. T.; Luther, J. M.; Ginsberg, N. S. Heterogeneous Charge Carrier Dynamics in Organic-Inorganic Hybrid Materials: Nanoscale Lateral and Depth-Dependent Variation of Recombination Rates in Methylammonium Lead Halide Perovskite Thin Films. *Nano Lett.* **2015**, *15*, 4799−4807.

(21) Stewart, R. J.; Grieco, C.; Larsen, A. V.; Maier, J. J.; Asbury, J. B. Approaching Bulk Carrier Dynamics in Organo-Halide Perovskite Nanocrystalline Films by Surface Passivation. *J. Phys. Chem. Lett.* **2016**, *7*, 1148−1153.

(22) Aberle, A. G. Surface Passivation of Crystalline Silicon Solar Cells: A Review. *Prog. Photovoltaics* **2000**, *8*, 473−487.

(23) Bertness, K. A.; Kurtz, S. R.; Friedman, D. J.; Kibbler, A. E.; Kramer, C.; Olson, J. M. 29.5%-Efficient GaInP/GaAs Tandem Solar Cells. *Appl. Phys. Lett.* **1994**, *65*, 989−991.

(24) Sheldon, M. T.; Eisler, C. N.; Atwater, H. A. GaAs Passivation with Trioctylphosphine Sulfide for Enhanced Solar Cell Efficiency and Durability. *Adv. Energy Mater.* **2012**, *2*, 339−344.

(25) Tang, J.; Kemp, K. W.; Hoogland, S.; Jeong, K. S.; Liu, H.; Levina, L.; Furukawa, M.; Wang, X.; Debnath, R.; Cha, D.; et al. Colloidal-Quantum-Dot Photovoltaics Using Atomic-Ligand Passivation. *Nat. Mater.* **2011**, *10*, 765−771.

(26) Boles, M. A.; Ling, D.; Hyeon, T.; Talapin, D. V. The Surface Science of Nanocrystals. *Nat. Mater.* **2016**, *15*, 141−153.

(27) Munro, A. M.; Jen-La Plante, I.; Ng, M. S.; Ginger, D. S. Quantitative Study of the Effects of Surface Ligand Concentration on CdSe Nanocrystal Photoluminescence. *J. Phys. Chem. C* **2007**, *111*, 6220−6227.

(28) Colbert, A. E.; Wu, W.; Janke, E. M.; Ma, F.; Ginger, D. S. Effects of Ligands on Charge Generation and Recombination in Hybrid Polymer/Quantum Dot Solar Cells. *J. Phys. Chem. C* **2015**, *119*, 24733−24739.

(29) Peterson, M. D.; Cass, L. C.; Harris, R. D.; Edme, K.; Sung, K.; Weiss, E. A. The Role of Ligands in Determining the Exciton Relaxation Dynamics in Semiconductor Quantum Dots. *Annu. Rev. Phys. Chem.* **2014**, *65*, 317−339.

(30) Lee, J. W.; Kim, H. S.; Park, N. G. Lewis Acid-Base Adduct Approach for High Efficiency Perovskite Solar Cells. *Acc. Chem. Res.* **2016**, *49*, 311−319.

(31) De Marco, N.; Zhou, H.; Chen, Q.; Sun, P.; Liu, Z.; Meng, L.; Yao, E. P.; Liu, Y.; Schiffer, A.; Yang, Y. Guanidinium: A Route to Enhanced Carrier Lifetime and Open-Circuit Voltage in Hybrid Perovskite Solar Cells. *Nano Lett.* **2016**, *16*, 1009−1016.

(32) Li, X.; Ibrahim Dar, M.; Yi, C.; Luo, J.; Tschumi, M.; Zakeeruddin, S. M.; Nazeeruddin, M. K.; Han, H.; Gratzel, M. Improved Performance and Stability of Perovskite Solar Cells by Crystal Crosslinking with Alkylphosphonic Acid ω-Ammonium Chlorides. *Nat. Chem.* **2015**, *7*, 703−711.

(33) Ahn, N.; Son, D. Y.; Jang, I. H.; Kang, S. M.; Choi, M.; Park, N. G. Highly Reproducible Perovskite Solar Cells with Average Efficiency

DOI: 10.1021/acsenergylett.6b00236
ACS Energy Lett. 2016, 1, 438−444

of 18.3% and Best Efficiency of 19.7% Fabricated via Lewis Base Adduct of Lead(II) Iodide. *J. Am. Chem. Soc.* **2015**, *137*, 8696−8699.
(34) Chen, Q.; Zhou, H.; Song, T. B.; Luo, S.; Hong, Z.; Duan, H. S.; Dou, L.; Liu, Y.; Yang, Y. Controllable Self-Induced Passivation of Hybrid Lead Iodide Perovskites Toward High Performance Solar Cells. *Nano Lett.* **2014**, *14*, 4158−4163.
(35) Zhang, W.; Saliba, M.; Moore, D. T.; Pathak, S. K.; Horantner, M. T.; Stergiopoulos, T.; Stranks, S. D.; Eperon, G. E.; Alexander-Webber, J. A.; Abate, A.; et al. Ultrasmooth Organic-Inorganic Perovskite Thin-Film Formation and Crystallization for Efficient Planar Heterojunction Solar Cells. *Nat. Commun.* **2015**, *6*, 6142.
(36) Eperon, G. E.; Habisreutinger, S. N.; Leijtens, T.; Bruijnaers, B. J.; van Franeker, J. J.; deQuilettes, D. W.; Pathak, S.; Sutton, R. J.; Grancini, G.; Ginger, D. S.; et al. The Importance of Moisture in Hybrid Lead Halide Perovskite Thin Film Fabrication. *ACS Nano* **2015**, *9*, 9380−9393.
(37) Tian, Y.; Peter, M.; Unger, E. L.; Abdellah, M.; Zheng, K.; Pullerits, T.; Yartsev, A.; Sundstrom, V.; Scheblykin, I. Mechanistic Insights into Perovskite Photoluminescence Enhancement: Light Curing with Oxygen Can Boost Yield Thousandfold. *Phys. Chem. Chem. Phys.* **2015**, *17*, 24978−24987.
(38) Galisteo-Lopez, J. F.; Anaya, M.; Calvo, M. E.; Miguez, H. Environmental Effects on the Photophysics of Organic-Inorganic Halide Perovskites. *J. Phys. Chem. Lett.* **2015**, *6*, 2200−2205.
(39) Yamada, Y.; Nakamura, T.; Endo, M.; Wakamiya, A.; Kanemitsu, Y. Photocarrier Recombination Dynamics in Perovskite $CH_3NH_3PbI_3$ for Solar Cell Applications. *J. Am. Chem. Soc.* **2014**, *136*, 11610−11613.
(40) Sakai, N.; Pathak, S.; Chen, H.-W.; Haghighirad, A. A.; Stranks, S. D.; Miyasaka, T.; Snaith, H. J. The Mechanism of Toluene-Assisted Crystallization of Organic−Inorganic Perovskites for Highly Efficient Solar Cells. *J. Mater. Chem. A* **2016**, *4*, 4464−4471.
(41) Sanchez, P.; Fernández, B.; Menéndez, A.; Gómez, D.; Pereiro, R.; Sanz-Medel, A. A Path Towards a Better Characterisation of Silicon Thin-Film Solar Cells: Depth Profile Analysis by Pulsed Radio-frequency Glow Discharge Optical Emission Spectrometry. *Prog. Photovoltaics* **2013**, *22*, 1246−1255.
(42) Dharmadasa, I. M.; Ives, M.; Brooks, J. S.; France, G. H.; Brown, S. J. Application of Glow Discharge Optical Emission Spectroscopy to Study Semiconductors and Semiconductor Devices. *Semicond. Sci. Technol.* **1995**, *10*, 369−372.
(43) Anderson, N. C.; Owen, J. S. Soluble, Chloride-Terminated CdSe Nanocrystals: Ligand Exchange Monitored by ^{1}H and ^{31}P NMR Spectroscopy. *Chem. Mater.* **2013**, *25*, 69−76.
(44) Kuhl, O. *Phosphorus-31 NMR Spectroscopy: A Concise Introduction for the Synthetic Organic and Organometallic Chemist*; Springer Verlag: Berlin, 2008.
(45) Stranks, S. D.; Eperon, G. E.; Grancini, G.; Menelaou, C.; Alcocer, M. J. P.; Leijtens, T.; Herz, L. M.; Petrozza, A.; Snaith, H. J. Electron-Hole Diffusion Lengths Exceeding 1 Micrometer in an Organometal Trihalide Perovskite Absorber. *Science* **2013**, *342*, 341−344.
(46) Eperon, G. E.; Stranks, S. D.; Menelaou, C.; Johnston, M. B.; Herz, L. M.; Snaith, H. J. Formamidinium Lead Trihalide: A Broadly Tunable Perovskite for Efficient Planar Heterojunction Solar Cells. *Energy Environ. Sci.* **2014**, *7*, 982−988.
(47) Vrućinić, M.; Matthiesen, C.; Sadhanala, A.; Divitini, G.; Cacovich, S.; Dutton, S. E.; Ducati, C.; Atatüre, M.; Snaith, H.; Friend, R. H.; et al. Local Versus Long-Range Diffusion Effects of Photoexcited States on Radiative Recombination in Organic-Inorganic Lead Halide Perovskites. *Adv. Sci.* **2015**, *2*, 1500136.
(48) Draguta, S.; Thakur, S.; Morozov, Y. V.; Wang, Y.; Manser, J. S.; Kamat, P. V.; Kuno, M. Spatially Non-uniform Trap State Densities in Solution-Processed Hybrid Perovskite Thin Films. *J. Phys. Chem. Lett.* **2016**, *7*, 715−721.
(49) Tian, Y.; Merdasa, A.; Unger, E.; Abdellah, M.; Zheng, K.; McKibbin, S.; Mikkelsen, A.; Pullerits, T.; Yartsev, A.; Sundstrom, V.; et al. Enhanced Organo-Metal Halide Perovskite Photoluminescence from Nanosized Defect-Free Crystallites and Emitting Sites. *J. Phys. Chem. Lett.* **2015**, *6*, 4171−4177.
(50) Tian, Y.; Merdasa, A.; Peter, M.; Abdellah, M.; Zheng, K.; Ponseca, C. S., Jr.; Pullerits, T.; Yartsev, A.; Sundstrom, V.; Scheblykin, I. G. Giant Photoluminescence Blinking of Perovskite Nanocrystals Reveals Single-Trap Control of Luminescence. *Nano Lett.* **2015**, *15*, 1603−1608.
(51) Lindsey, C. P.; Patterson, G. D. Detailed Comparison of the Williams−Watts and Cole−Davidson Functions. *J. Chem. Phys.* **1980**, *73*, 3348−3357.
(52) Johnston, M. B.; Herz, L. M. Hybrid Perovskites for Photovoltaics: Charge-Carrier Recombination, Diffusion, and Radiative Efficiencies. *Acc. Chem. Res.* **2016**, *49*, 146−154.
(53) Milot, R. L.; Eperon, G. E.; Snaith, H. J.; Johnston, M. B.; Herz, L. M. Temperature-Dependent Charge-Carrier Dynamics in $CH_3NH_3PbI_3$ Perovskite Thin Films. *Adv. Funct. Mater.* **2015**, *25*, 6218−6227.
(54) Saba, M.; Cadelano, M.; Marongiu, D.; Chen, F.; Sarritzu, V.; Sestu, N.; Figus, C.; Aresti, M.; Piras, R.; Lehmann, A. G.; et al. Correlated Electron-Hole Plasma in Organometal Perovskites. *Nat. Commun.* **2014**, *5*, 5049.
(55) Nie, W.; Tsai, H.; Asadpour, R.; Blancon, J. C.; Neukirch, A. J.; Gupta, G.; Crochet, J. J.; Chhowalla, M.; Tretiak, S.; Alam, M. A.; et al. High-Efficiency Solution-Processed Perovskite Solar Cells with Millimeter-Scale Grains. *Science* **2015**, *347*, 522−525.
(56) Yamada, Y.; Yamada, T.; Phuong, L. Q.; Maruyama, N.; Nishimura, H.; Wakamiya, A.; Murata, Y.; Kanemitsu, Y. Dynamic Optical Properties of $CH_3NH_3PbI_3$ Single Crystals As Revealed by One- and Two-Photon Excited Photoluminescence Measurements. *J. Am. Chem. Soc.* **2015**, *137*, 10456−10459.
(57) Pazos-Outon, L. M.; Szumilo, M.; Lamboll, R.; Richter, J. M.; Crespo-Quesada, M.; Abdi-Jalebi, M.; Beeson, H. J.; Vrućinić, M.; Alsari, M.; Snaith, H. J.; et al. Photon Recycling in Lead Iodide Perovskite Solar Cells. *Science* **2016**, *351*, 1430−1433.
(58) Leblebici, S. Y.; Leppert, L.; Li, Y.; Reyes-Lillo, S. E.; Wickenburg, S.; Wong, E.; Lee, J.; Melli, M.; Ziegler, D.; Angell, D. K.; et al. Facet-Dependent Photovoltaic Efficiency Variations in Single Grains of Hybrid Halide Perovskite. *Nat. Energy* **2016**, *1*, 16093.
(59) Green, M. A. Radiative Efficiency of State-of-the-Art Photovoltaic Cells. *Prog. Photovoltaics* **2012**, *20*, 472−476.
(60) Miller, O. D.; Yablonovitch, E.; Kurtz, S. R. Strong Internal and External Luminescence as Solar Cells Approach the Shockley-Queisser Limit. *IEEE J. Photovolt.* **2012**, *2*, 303−311.
(61) Braly, I. L.; Hillhouse, H. W. Optoelectronic Quality and Stability of Hybrid Perovskites from $MAPbI_3$ to $MAPbI_2Br$ Using Composition Spread Libraries. *J. Phys. Chem. C* **2016**, *120*, 893−902.
(62) Sutter-Fella, C. M.; Li, Y.; Amani, M.; Ager, J. W., 3rd; Toma, F. M.; Yablonovitch, E.; Sharp, I. D.; Javey, A. High Photoluminescence Quantum Yield in Band Gap Tunable Bromide Containing Mixed Halide Perovskites. *Nano Lett.* **2016**, *16*, 800−806.

DOI: 10.1021/acsenergylett.6b00236
ACS Energy Lett. 2016, 1, 438−444